Scientific Research Publishing

World Journal of Engineering and Technology, 2025, 13(3), 607-621
https://www.scirp.org/journal/wjet
ISSN Online: 2331-4249
ISSN Print: 2331-4222

Design and Implementation of a UAV Platform for Educational Applications: A Multi-Disciplinary Engineering Approach

Hussien Elharati[1], Abdulhamid Zaidi[2], Mohamad Izdin Hlal[3], Mickelange Prince[1], Omar Beg[1]

[1]Department of Electrical Engineering, College of Engineering & Sciences, The University of Texas Permian Basin, Odessa, TX, USA
[2]Electrical and Computer Engineering Technology, Indiana State University, Terre Haute, IN, USA
[3]Department of Electrical Engineering, Higher Institute of Science and Technology, Souk Aljum'aa, Libya
Email: eharati_h@utpb.edu, Abdulhamid.zaidi@indstate.edu, mohamadizdinhlal@yahoo.com, prince_m59312@utpb.edu, beg_o@utpb.edu

How to cite this paper: Elharati, H., Zaidi, A., Hlal, M.I., Prince, M. and Beg, O. (2025) Design and Implementation of a UAV Platform for Educational Applications: A Multi-Disciplinary Engineering Approach. *World Journal of Engineering and Technology*, **13**, 607-621.
https://doi.org/10.4236/wjet.2025.133039

Received: July 4, 2025
Accepted: August 19, 2025
Published: August 22, 2025

Abstract

The contemporary educational landscape is increasingly shaped by the need to align with rapid technological advancements. This calls for a reevaluation of academic programs and a focus on cultivating adaptable, skilled individuals capable of meeting evolving industrial demands. This paper presents the design, development, and experimental evaluation of a low-cost Unmanned Aerial Vehicle (UAV) based on the Arduino microcontroller platform. The UAV system comprises key components such as an inertial measurement unit (IMU), electronic speed controllers (ESCs), and brushless DC motors, all governed by a custom-built Arduino-based flight controller. The design emphasizes modularity, affordability, and ease of replication, rendering it highly suitable for educational and research purposes. Detailed discussions are provided on the system architecture, sensor integration, flight control algorithms, and wireless communication mechanisms. Experimental testing, corroborated by simulation, demonstrates that the UAV achieves a payload capacity of approximately 0.6 kg, which meets the design objectives. The project offers a practical, interdisciplinary learning platform, equipping students with essential competencies in embedded systems, control engineering, and mechatronic system integration skills that are directly transferable to contemporary engineering practice.

Keywords

Unmanned Aerial Vehicle (UAV), SolidWorks, Flight Controller, Proportional-Integral-Derivative (PID), Microcontroller, Six Degrees of Freedom (6-DOF)

1. Introduction

Unmanned Aerial Vehicles (UAVs), commonly known as drones, have revolutionized multiple sectors by offering innovative solutions in areas such as environmental monitoring, agriculture, infrastructure inspection, search and rescue operations, and aerial mapping [1] [2]. As UAV technologies continue to evolve, there is a growing demand for low-cost, modular, and customizable systems that can be tailored to specific applications and educational needs [3]. The development of such systems presents an ideal opportunity for engineering students to engage in hands-on learning experiences that integrate concepts across multiple disciplines.

In recent years, Arduino-based platforms have gained popularity for their accessibility, open-source nature, and ease of integration with a wide variety of sensors and actuators [4]. Arduino microcontrollers are particularly well-suited for UAV development due to their low cost, flexibility, and active support community, making them an excellent choice for academic and prototyping purposes [5]. By combining Arduino-based control systems with lightweight mechanical frames, students can create functioning UAVs that serve both educational and practical purposes.

Engineering capstone projects provide a critical opportunity for senior undergraduate students to apply theoretical knowledge in a real-world context. These projects often aim to emulate the professional engineering design process, from requirements gathering and conceptual design to prototyping, testing, and iteration [6]. Capstone courses are increasingly adopting interdisciplinary approaches, encouraging collaboration between electrical, mechanical, and computer engineering students to address complex systems level problems [7]. UAV systems, with their integration of aerodynamics, structural mechanics, electronics, embedded programming, and control systems, offer a compelling platform for such interdisciplinary collaboration. There are various categories of drones, which differ according to their structure and use, as well as various ways of controlling. The main categories are based on their construction and the different flight and lifting techniques [8], as shown in **Figure 1**.

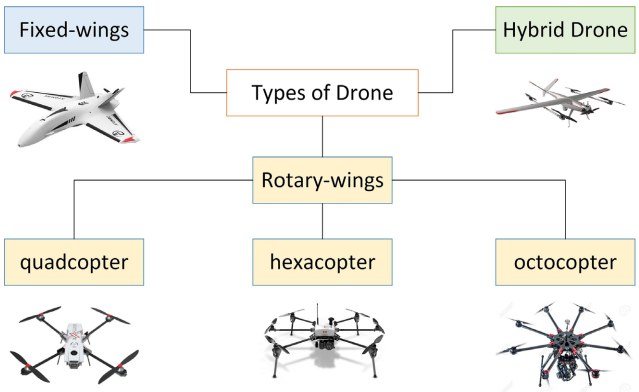

Figure 1. UAV main categories based on construction, different flight and lifting techniques.

This paper presents the design and implementation of a quadcopter UAV system developed using Arduino microcontrollers as the central flight control unit. The project was undertaken as part of a senior interdisciplinary capstone course at UTPB combining Electrical and Mechanical Engineering curricula. The electrical subsystem included sensor integration, power distribution, and wireless communication, while the mechanical subsystem focused on frame design, motor mounting, and weight optimization. Emphasis was placed on system modularity, cost efficiency, and educational value to ensure replicability for future student teams.

The objectives of this paper are threefold: 1) to describe the detailed design methodology and implementation strategy for a functional, low-cost UAV system using Arduino-based components; 2) to highlight the interdisciplinary collaboration involved in integrating electrical and mechanical subsystems; and 3) to evaluate the system's performance through field testing and iterative refinement. By documenting this process, the paper contributes to the growing body of literature on project-based learning and low-cost UAV development and offers practical guidance for similar educational initiatives.

The course breaks building a quadcopter into four high-level tasks: dynamic analysis (mathematical analysis, Kinematic Modeling, Dynamic Modeling), Structure of Quadcopter (Frame design, Electronic and mechanical components), Simulation and Results, and getting the quadcopter flying. Below we describe each of these tasks and the key challenges they present for the students and the course staff.

2. Dynamic Analysis

Movement of the quadcopter depends exclusively on four electric motors located symmetrically at its edge as shown in Figure 2.

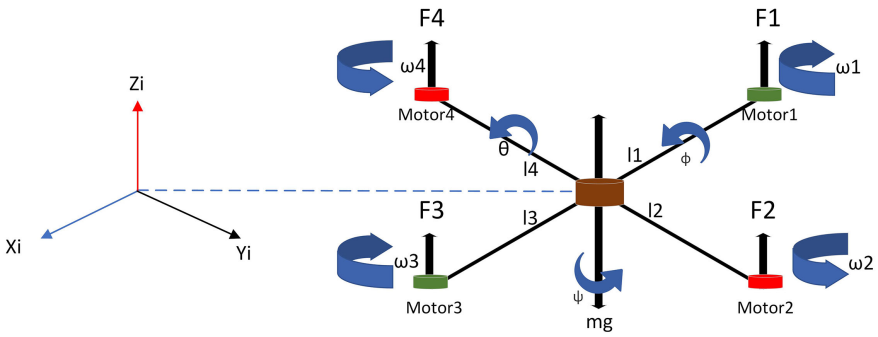

a. Inertial frame

b. body frame

Figure 2. Quadcopter inertial and body frames.

The quadcopter takes place when the upward lift force produced by all four engines will overcome the force of gravity. Therefore, in the case of lifting, all four electric motors must have the same angular velocity with lift force greater than the force of gravity. To achieve the x-axis rotation (Roll), there must be changes

in the angular velocities of the four motors, right rotation (roll right) is achieved if the angular velocities of motors "3" and "4" are increased and "1" and "2" remain constant. On the contrary, left rotation requires an increase in the speeds of motors "1" and "2" and stability of "3" and "4". Regarding the rotation along the y-axis (Pitch) and for the positive elevation rotation (pitch up) and the negative elevation rotation (pitch down), the speeds of motors "2" and "3", and the angular speeds of motors "1" and "4" should be increased respectively each time. In case the movement is made with respect to the deflection z-axis (Yaw), changes in the speed of the motors are required, specifically, for right displacement, the angular velocities of motors "2" and "4" should be increased with the other two "1" and "3" fixed. For left displacement, the velocities of "1" and "3" are increased and those of "2" and "4" remain fixed [9].

2.1. Mathematical Analysis

The quadcopter mathematical analysis is carried out based on the laws of physics and mechanics [10]. The mathematical model considers two axis reference systems, as shown in **Figure 2**. The first coordinate system is the inertial frame [x_i, y_i, z_i] which is fixed to ground, while the second is the body frame [x_b, y_b, z_b] which is considered as a part of the quadcopter attached to the center of mass of the quadcopter [11]. The angular velocities of the motors are represented by ω_1, ω_2, ω_3, and ω_4, which generate the forces F_1, F_2, F_3, and F_4, respectively.

The six motions along the six degrees of freedom (DOF) of the quadcopter in the 3D space (x, y, z) include the translational motions (longitudinal $\dot{x}$, lateral $\dot{y}$, and vertical $\dot{z}$), and the rotational motions (roll $\dot{p}$, pitch $\dot{q}$, and yaw $\dot{r}$), respectively. The quadcopter motion was analyzed according to the length of the arms (ℓ_1, ℓ_2, ℓ_3, and ℓ_4). The differences in the angular velocity of the motors (ω_1, ω_2, ω_3 and ω_4) result in the motions along x, y, and z-axes. The difference in ω_1 and ω_3 causes the roll motion $\dot{p}$, while the difference in ω_2 and ω_4 causes the pitch motion $\dot{q}$. The vertical motion along z-axis and the yaw motion $\dot{r}$ are caused by the rotational directions of all motors [12].

2.1.1. Kinematic Modeling

The following mathematical equation describes the motion of a rigid body in space which relates to the inertial frame and body fixed frame under the action of external forces. The transformation matrix R between the frames is obtained by the consecutive rotations; roll φ, pitch θ, and yaw ψ (Euler's angle) about x, y and z axes, as given in Equations (1)-(3) [13].

$$\begin{Bmatrix} \ddot{x} \\ \ddot{y} \\ \ddot{z} \end{Bmatrix} = R * \begin{Bmatrix} \dot{x} \\ \dot{y} \\ \dot{z} \end{Bmatrix} \tag{1}$$

$$R = \begin{pmatrix} \cos\theta\cos\psi & \sin\phi\sin\theta\cos\psi - \cos\phi\sin\psi & \cos\phi\sin\theta\cos\psi + \sin\phi\sin\psi \\ \cos\theta\sin\psi & \sin\phi\sin\theta\sin\psi - \cos\phi\sin\psi & \sin\phi\sin\theta\sin\psi - \cos\phi\cos\psi \\ -\sin\theta & \sin\phi\cos\theta & \cos\phi\cos\theta \end{pmatrix} \tag{2}$$

$$\begin{pmatrix} \dot{\varphi} \\ \dot{\theta} \\ \dot{\psi} \end{pmatrix} = \begin{pmatrix} 1 & \tan\theta\sin\theta & \tan\theta\cos\theta \\ 0 & \cos\theta & -\sin\phi \\ 0 & \dfrac{\sin\phi}{\cos\theta} & \dfrac{\cos\varphi}{\cos\theta} \end{pmatrix} = \begin{pmatrix} \dot{p} \\ \dot{q} \\ \dot{r} \end{pmatrix} \tag{3}$$

where: R is the transformation matrix between the inertial frame and the body fixed frame; ψ, θ, and φ are Euler angles (z, y, x).

2.1.2. Dynamic Modeling

Dynamic model is obtained by analyzing various forces and torques. The upward forces F_1, F_2, F_3, and F_4 produced by the quad's motors yields resultant moments (torques) T_x, T_y, and T_z along body frame axes x, y and z [14], as explained in the following equations.

$$T_x = \ell\left(F_1 - F_3\right) \tag{4}$$

$$T_y = \ell\left(F_2 - F_4\right) \tag{5}$$

$$T_z = M_2 + M_4 - M_1 - M_3 \tag{6}$$

Based on the previous analysis, the following equations for the quadcopter's dynamic motion are derived:

$$\begin{cases} m\ddot{x} = \left(c\phi s\theta c\psi + s\phi s\psi\right) \\ m\ddot{y} = \left(c\phi s\theta s\psi + s\phi c\psi\right) \\ m\ddot{Z} = Fc\phi c\theta - mg \\ I_x\ddot{P} = T_x + \dot{q}\dot{r}\left(I_y - I_z\right) \\ I_y\ddot{q} = T_y + \dot{r}\dot{p}\left(I_z - I_x\right) \\ I_z\ddot{r} = T_z + \dot{p}\dot{q}\left(I_x - I_y\right) \end{cases} \tag{7}$$

3. Control Algorithm

The PID controller is implemented by optimizing P, I and D parameters against the errors as shown in **Figure 3**. PID is the most widespread type of industrial control due to its ease of adjustment, low cost and high performance in most practical systems [15] [16]. To achieve the desired accuracy, the equations of motion are used to develop model-based to control 6-degrees of freedom in 3-dimensional space quadcopter. The following MATLAB codes demonstrate the control strategy proposed for the altitude and attitude of the angular speeds (inputs) to the four propellers.

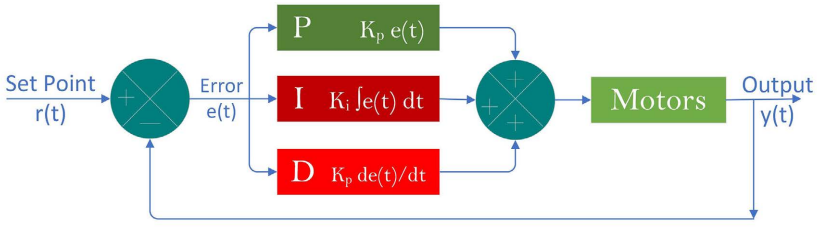

Figure 3. A typical closed-loop system.

//Compute errors

//Roll calculations

pid_error = gyro_roll_input – pid_roll_setpoint;

*pid_roll = pid_k$_p$_roll * pid_error + pid_k$_i$_roll + pid_k$_d$_roll * (pid_error - pid_last_roll_k$_d$_error);*

//Pitch calculations

pid_error = gyro_pitch_input – pid_pitch_setpoint;

*pid_pitch = pid_k$_p$_pitch * pid_error + pid_k$_i$_pitch + pid_k$_d$_pitch * (pid_error - pid_last_pitch_kd_error);*

//Yaw calculations

pid_error = gyro_yaw_input – pid_yaw_setpoint;

*pid_yaw = pid_k$_p$_yaw * pid_error + pid_k$_i$_yaw + pid_k$_d$_yaw * (pid_error – pid_last_yaw_d_error);*

4. Structure of Quadcopter

The Quadcopter Structure is divided into two main categories, frame design, and electrical and mechanical parts.

4.1. Frame Design

In this section, the quadcopter frame was designed and optimized from scratch. The objective was to create a structure capable of mounting motors and housing the receiver, gyroscope sensor, flight controller, and battery. As shown in **Figure 4**, the entire frame was designed using SOLIDWORKS software and 3D printed at UTPB Makerspace. Carbon fiber reinforced filament sheets (HJ450, 2 mm thick) were used to enhance the strength and stiffness of the base material, resulting in a more robust and resilient drone frame with improved impact resistance and bending strength.

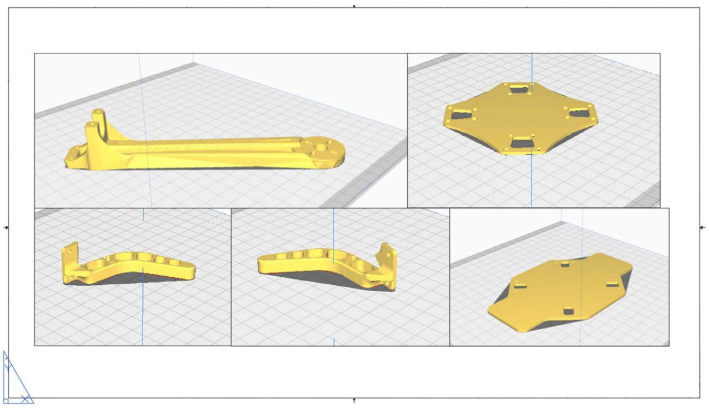

Figure 4. Frame design in SolidWorks.

4.2. Components

The development and assembly of the quadcopter system require the integration of several key electrical, electronic, and mechanical components. Each component

plays a specific role in ensuring flight stability, responsiveness, and operational efficiency. As shown in Figure 5, the major components and their specifications are described below.

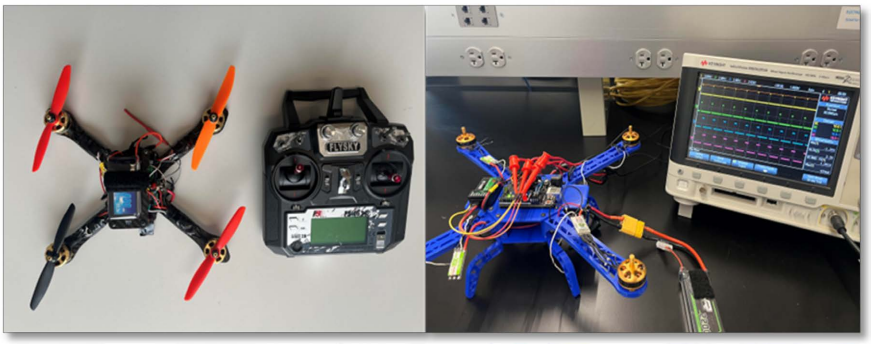

(a) (b)

Figure 5. (a) quadcopter system; (b) Pulse width modulation.

Flight Controller: The Arduino UNO, powered by the ATmega328 microcontroller, is employed as the flight controller (FC) due to its versatility, ease of programming, and availability of open-source resources. The FC is responsible for interpreting user commands Roll, Pitch, Throttle, and Yaw received via the receiver module. It processes sensor data to maintain flight stability by generating appropriate control signals for the Electronic Speed Controllers (ESCs) and motors. The controller also interfaces with an inertial measurement unit (IMU) to receive real-time orientation feedback through accelerometer and gyroscope data.

Brushless DC motors (BLDC): The propulsion system utilizes brushless DC motors rated at 1000 KV (1000 RPM for every volt), with each motor capable of delivering a thrust of approximately 900 g at 80% efficiency. The motors operate within a voltage range of 7 - 12 V and can handle a current draw of up to 12 A per minute. BLDC motors are preferred for UAV applications due to their high torque-to-weight ratio, low operational noise, high reliability, and long service life.

Electronic Speed Controllers (ESCs): Each motor is paired with a dedicated ESC, which regulates the motor's speed and direction based on the PWM signals received from the flight controller. The ESCs used in this configuration are rated for 30A output current and are powered by a 2 - 4 cell lithium-polymer (Li-Po) battery. The physical dimensions of each ESC are 45 mm × 24 mm × 11 mm, with an approximate weight of 25 g. These units convert digital control signals into the precise electrical outputs needed to drive the motors, as shown in Figure 5(b).

Gyro and Accelerometer: The MPU6050 sensor integrates a 3-axis gyroscope and a 3-axis accelerometer in a single compact, low-power chip. This module provides real-time motion and orientation data to the flight controller. The accelerometer detects linear acceleration and changes in movement direction, while the gyroscope measures angular velocity, allowing the system to respond accurately to deviations in orientation during flight.

Remote Control System: A 6-channel FS-i6X radio transmitter operating at 2.4 GHz is used to remotely control the quadcopter. The corresponding receiver module receives user input signals and transmits them to the flight controller. At a minimum, four control channels are required (Pitch, Roll, Throttle, and Yaw) for effective manual control of the quadcopter. The wireless communication system ensures reliable, real-time interaction between the user and the UAV, as shown in Figure 5(a).

Power Supply (Li-Po Battery): The quadcopter is powered by an 11.1 V, 2200 mAh lithium-polymer (Li-Po) battery. The battery has a weight of approximately 155 g and dimensions of 100 mm × 20 mm × 30 mm. Li-Po batteries are widely adopted in drone applications due to their high energy density, lightweight construction, high discharge rates, and extended runtime, making them suitable for high-performance aerial systems.

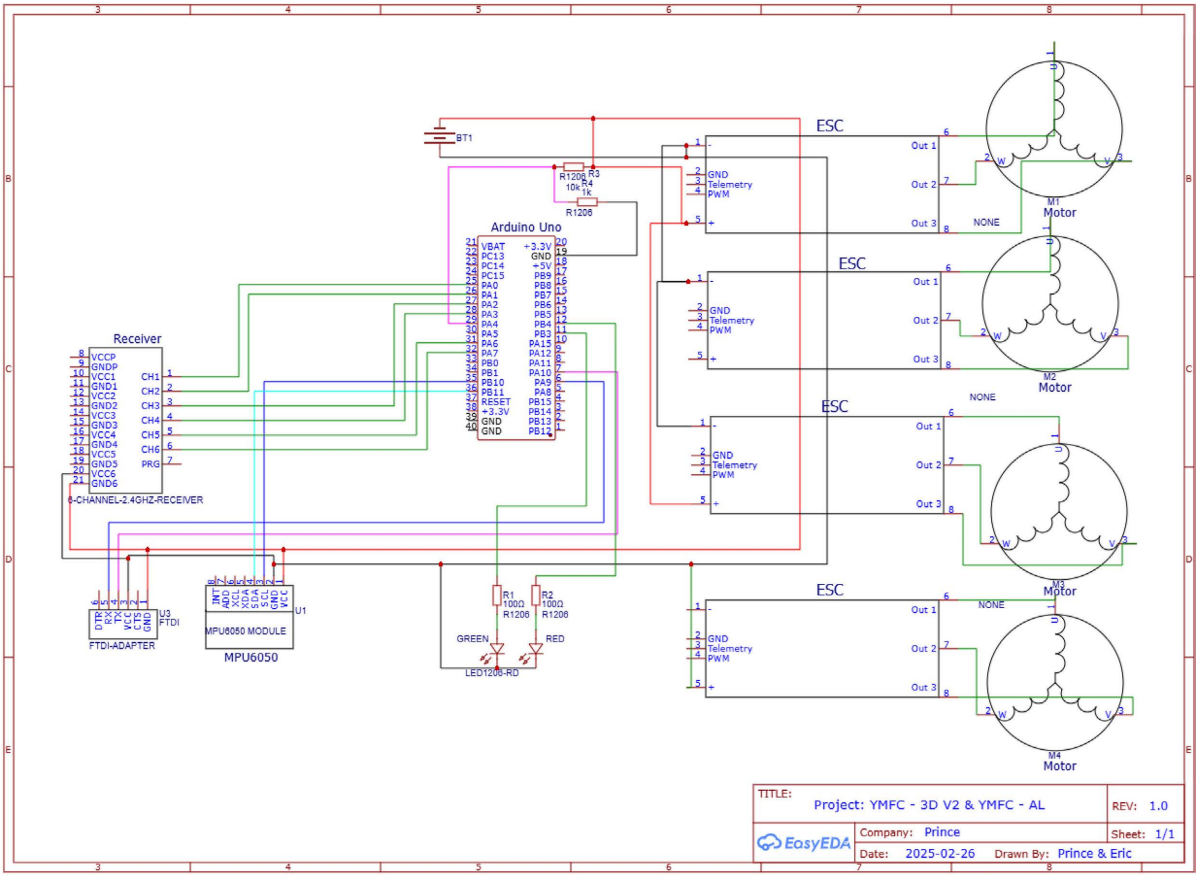

Figure 6. Quadcopter schematic diagram.

Propellers: The quadcopter uses 10-inch (25.4 cm) diameter propellers with a 4.5-inch pitch, each weighing around 7 g. Propellers serve the critical function of converting motor rotation into thrust. The choice of propeller size depends on the application: smaller propellers (less than 8 inches) are generally used for high-speed racing drones, while larger propellers (greater than 8 inches) are preferred for drones tasked with carrying payloads. The schematic and wiring diagram

showing the circuit connections are presented in Figure 6, while the complete circuit board layout of the quadcopter system is illustrated in Figure 7.

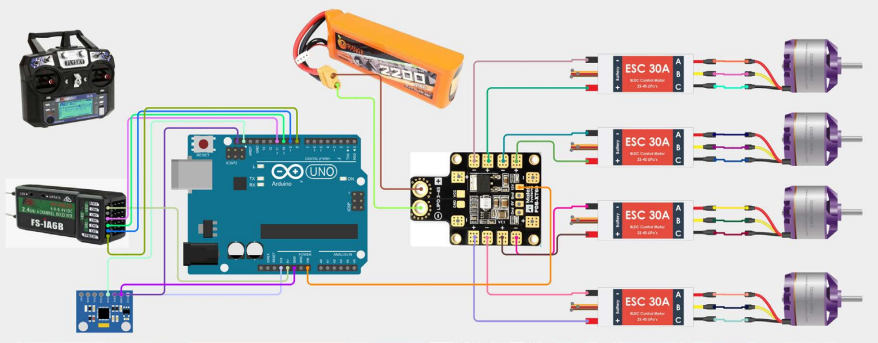

Figure 7. Quadcopter complete system.

5. Simulation and Results

A simulation environment was developed using MATLAB and Simulink (version R2024a, released March 20, 2024). Simulink provides a graphical interface for modeling, simulating, and analyzing dynamic systems without the need for manual coding. It supports the development of multidomain models, offering a clear visualization of system dynamics and signal flow, which enhances both model clarity and simulation fidelity. The parameter values used for the quadcopter model in the simulation framework are shown in Figure 8.

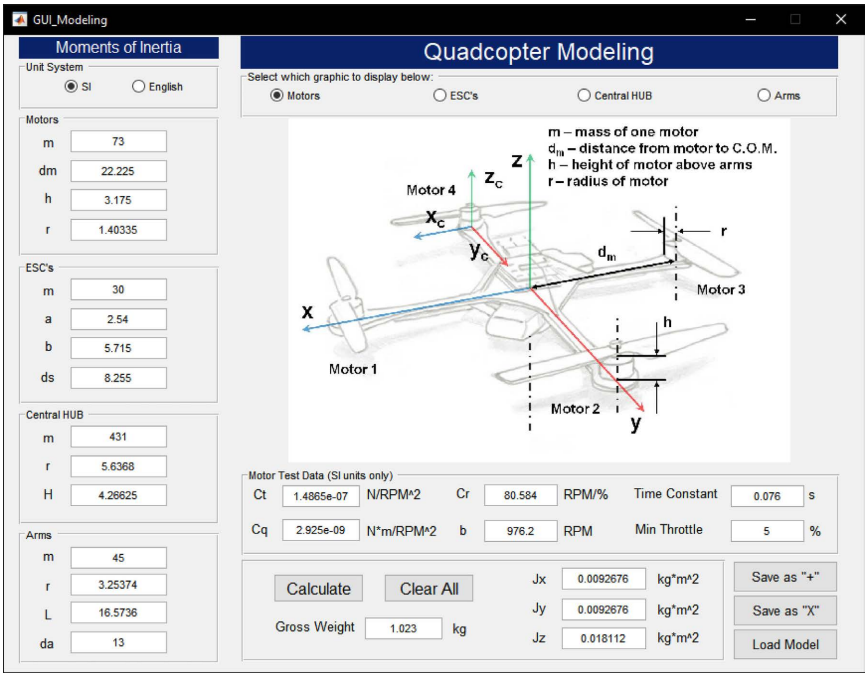

Figure 8. Quadcopter modeling and their parameters.

5.1. PID Controller

The closed-loop flight controller model was linearized around a hover condition

and subsequently simulated using the full-order nonlinear quadcopter model. In the simulation framework, the overall system is partitioned into two main subsystems: the Flight Controller and the Quadcopter System. The Flight Controller is responsible for managing translational position, attitude/altitude, and angular rate. It computes control inputs (U1, U2, U3, U4) based on the error signals obtained from the difference between the desired and current states. These control inputs are then applied to the Quadcopter System block, which encapsulates the system dynamics and control equations necessary for simulating the physical behavior of the quadcopter. The architecture of this model is illustrated in Figure 9.

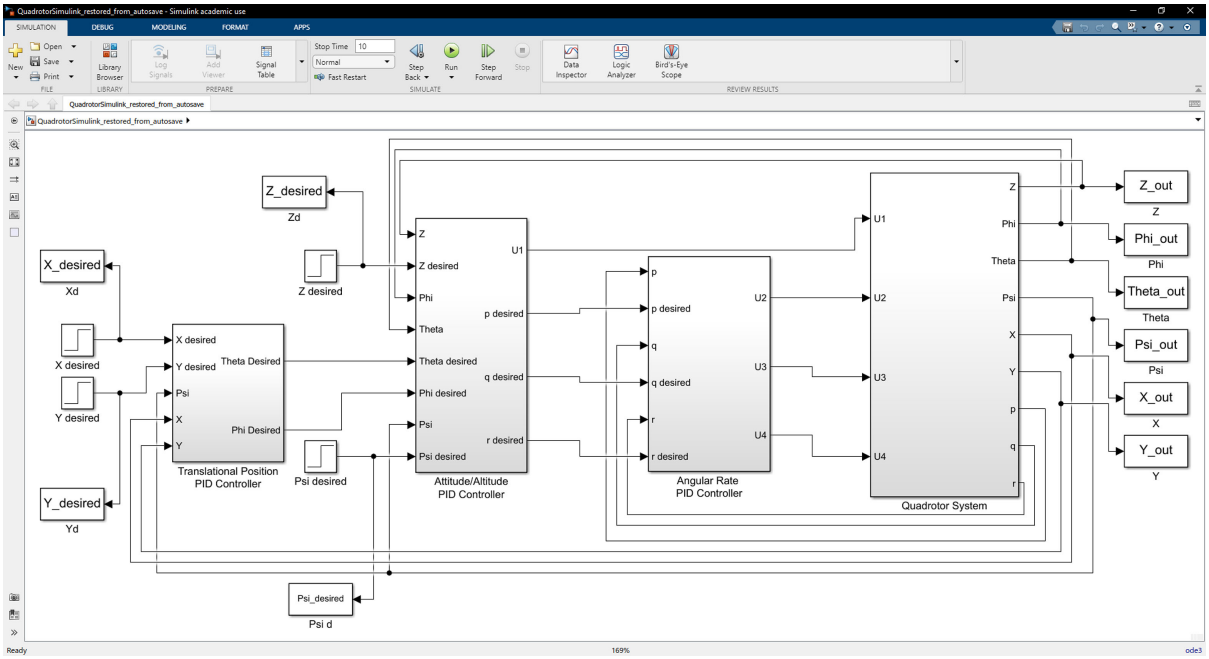

Figure 9. Quadcopter flight controller.

The combined effect of the proportional, integral, and derivative (PID) controller actions is represented by the following transfer function:

$$C(s) = K_p\left(1+1\frac{1}{T_i S}+T_d S\right) \tag{8}$$

$$u(s) = K_p\left[r(s)-y(s)+\frac{1}{sT_i}\left(r(s)-y(s)\right)+\frac{sT_d}{1+\frac{sT_d}{N}}\left(r(s)-y(s)\right)\right] \tag{9}$$

where: $r(s)$, $y(s)$ and $u(s)$ is the Laplace transform of the reference, process and control signal; K_p is the proportional gain; K_p/T_i is the integral gain; K_p T_d is the derivative gain; N is the ratio between T_d and the time constant.

The result was obtained from the linear model and flight path simulation of the aerial vehicle as shown in Figure 10. These results are based on a state-space representation linearized around a nominal operating point, such as hover or steady-level flight. Each plot presents a key aspect of the UAV's dynamic behavior and

validates the accuracy and performance of the derived linear model in predicting the system's response under small perturbations.

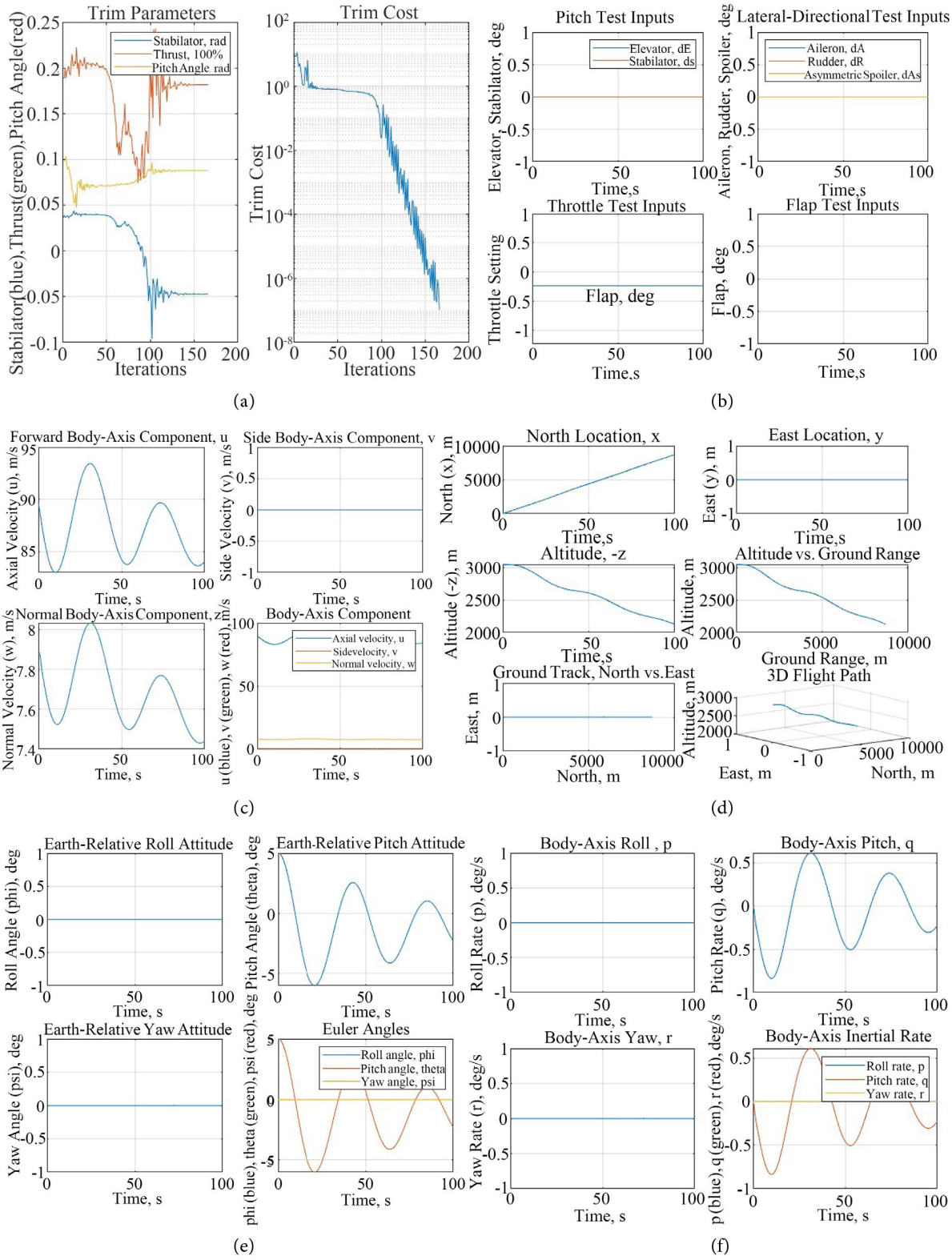

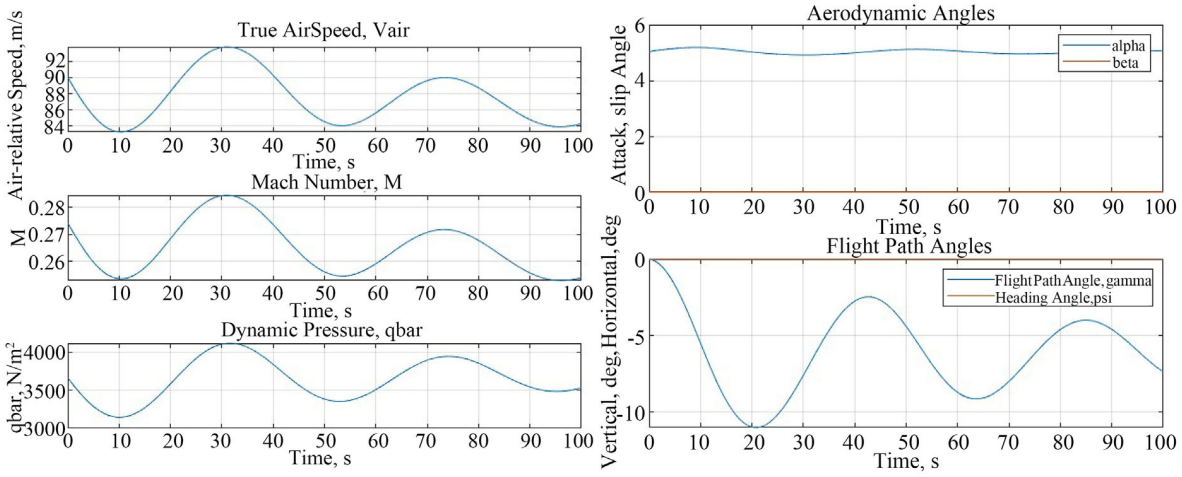

Figure 10. Linear Model, and Flight Path Simulation. (a) Trim Parameters vs Trim coast; (b) Pitch, lateral-direction, Throttle, Flap test inputs; (c) Inertial Velocity; (d) North, East, Attitude locations; (e) Inertial rate vector Components; (f) Earth relative and Euler Angles; (g) Air Speed, Mach Number and Dynamic Pressure; (h) Aerodynamic Angles vs Flight Path Angles.

Figure 11 presents the drone's trajectory tracking animation and showcases the integrated simulation of the Generic 6-DOF Trim, Linear Model, and Flight Path dynamics. It highlights the step response behavior of the Roll PID controller, which exhibits a noticeable overshoot and a settling time of approximately 4.5 seconds. The figure clearly illustrates the mismatch between the desired roll input and the actual measured roll response, emphasizing the limitations of the current PID tuning in the roll channel.

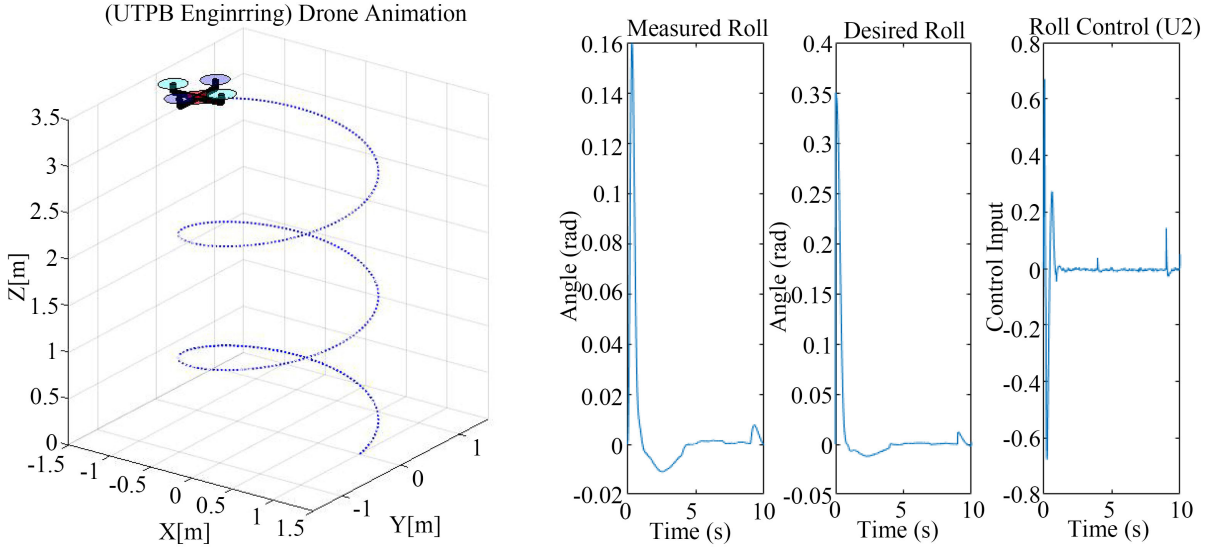

Figure 11. Drone trajectory tracking animation and step responses of Roll PID controller.

5.2. Flight Time Estimation

To estimate the flight time, thrust data from the motors was obtained through a

series of controlled experiments using an external power supply, a laser tachometer, and a clamp meter. The analysis assumes indoor flight conditions with low-speed operation, where the only external force considered is the thrust generated by the motor-propeller assembly; aerodynamic drag and wind effects are neglected. The laser tachometer measured the motors' rotational speed (RPM), while the clamp meter recorded the current drawn by each motor. These measurements established the relationship between input voltage, current consumption, and motor RPM, providing the basis for estimating total flight time and selecting a suitable battery. A summary of the experimental results is provided in Table 1.

Table 1. Voltage and thrust measuring observations.

Volt	*Current*	*PWM (%)*	*RPM*	*Weight (Kg)*	*Thrust*
1	2	15.5	2922	0.12	1.176
2	4	30.5	3920	0.34	4.312
3	7.5	49.0	4990	0.50	5.782
4	11.4	70.5	6820	0.77	6.86
5	16.6	98.9	7920	0.93	7.84

The experimental results indicate that the quadcopter operates effectively at approximately 50% PWM. At this level, each motor generates 0.5 kg of thrust, resulting in a total lift capacity of 2 kg (4 × 0.5 kg). Given that the quadcopter's total weight without payload is 1.4 kg, the estimated payload capacity is approximately 0.6 kg. At 50% PWM, the current drawn by each motor is 7.5 A, leading to a total current draw of 30 A (4 × 7.5 A). Using a 6 Ah battery, the estimated flight time is calculated as:

$$\text{Flight Time} = \frac{6 \times 60}{30} = 12 \text{ min}$$

The performance of the motor-propeller system is further analyzed by establishing the relationship between input voltage and output thrust. This relationship, obtained through curve fitting, is illustrated in Figure 12 and expressed in Equation (10):

$$F = 1.8V + 0.02 \tag{10}$$

where: F is the thrust force (in kg), V is the input voltage (in volts).

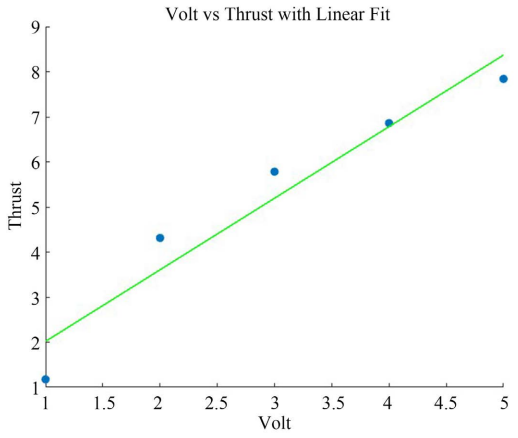

Figure 12. Input volt vs output thrust.

6. Conclusions

The objective of this research is to design a quadcopter based on the Arduino Uno microcontroller platform. We completed the custom design and constructed a UAV capable of performing specific tasks and carrying designated payloads. The project integrated concepts from electrical, electronic, and mechanical engineering, providing students with hands-on experience in designing and implementing complex systems. This practical knowledge is highly beneficial for students pursuing careers in engineering and research, particularly in the fields of electrical and mechanical engineering. As part of the design process, students utilized SolidWorks and a 3D-printer to fabricate the quadcopter chassis, that are capable of handling motors, sensors, and other essential components. The chassis was constructed using carbon fiber-reinforced filament sheets to ensure strength and durability.

Following the completion of the structural design, the flight control board was developed, integrated, and tested. Various experiments were conducted to validate the quadcopter's performance, including software installation, sensor initialization, radio signal reception, and Roll, Pitch, and Yaw calibration. Students also gained practical experience with ESCs, BLDC motors, the I2C protocol, and PID tuning. Experimental and simulation results confirm stable flight and an estimated payload capacity of approximately 0.6 kg, which is considered satisfactory. The proposed class structure is adaptable and can be tailored to align with the specific curricular needs of different academic institutions.

Conflicts of Interest

The authors declare no conflicts of interest regarding the publication of this paper.

References

[1] Zhang, C. and Kovacs, J.M. (2012) The Application of Small Unmanned Aerial Systems for Precision Agriculture: A Review. *Precision Agriculture*, **13**, 693-712. https://doi.org/10.1007/s11119-012-9274-5

[2] Pajares, G. (2015) Overview and Current Status of Remote Sensing Applications Based on Unmanned Aerial Vehicles (UAVS). *Photogrammetric Engineering & Remote Sensing*, **81**, 281-330. https://doi.org/10.14358/pers.81.4.281

[3] Mamchur, D. and Kolodinskis, A. (2025) Quadcopter Prototyping for Teaching University Students. *Evija Kļave*, 155.

[4] Banzi, M. and Shiloh, M. (2014) Getting Started with Arduino. 3rd Edition, Maker Media.

[5] Petriu, E.M., *et al.* (2014) Sensor-Based Information Processing for Autonomous Navigation Using Arduino Platforms. *IEEE Instrumentation & Measurement Magazine*, **17**, 14-22.

[6] Mohsan, S.A.H., *et al.* (2022) Towards the Unmanned Aerial Vehicles (UAVs): A Comprehensive Review. *Drones*, **6**, 147.

[7] Bryceson, K., *et al.* (2016) Small Quadcopter Drones as Educational Tools in Agriculture at the University of Queensland. *EDULEARN16 Proceedings*, IATED.

[8] Kim, T.H. and Lee, S.H. (2025) Development of HTOL, VTOL, Hybrid, and Unconventional UAV Systems: A Survey of Flight and Lift Mechanisms. Exploring Drone Classifications and Applications: A Review. ResearchGate.

[9] Nikitina, N.V. (2019) Stability Analysis of Rotary Motions of a Quadcopter. *International Applied Mechanics*, **55**, 648-653. https://doi.org/10.1007/s10778-019-00986-8

[10] Prasetia, A.S., Wai, R., Wen, Y. and Wang, Y. (2019) Mission-Based Energy Consumption Prediction of Multirotor UAV. *IEEE Access*, **7**, 33055-33063. https://doi.org/10.1109/access.2019.2903644

[11] Chen, J.I. and Lin, H. (2023) Performance Evaluation of a Quadcopter by an Optimized Proportional-Integral-Derivative Controller. *Applied Sciences*, **13**, Article 8663. https://doi.org/10.3390/app13158663

[12] Kumar, R., Deshpande, A.M., Wells, J.Z. and Kumar, M. (2020) Flight Control of Sliding Arm Quadcopter with Dynamic Structural Parameters. 2020 *IEEE/RSJ International Conference on Intelligent Robots and Systems* (*IROS*), Las Vegas, 24 October 2020-24 January 2021, 1358-1363. https://doi.org/10.1109/iros45743.2020.9340694

[13] Kumar, P., Ahmad, F. and Patil, P.P. (2021) Analysis of the Quadcopter Dynamics with Different Frame Structures. In: Kumar, N., Tibor, S., Sindhwani, R., Lee, J. and Srivastava, P., Eds., *Lecture Notes in Mechanical Engineering*, Springer Singapore, 681-688. https://doi.org/10.1007/978-981-15-9956-9_66

[14] Islam, M., Okasha, M. and Idres, M.M. (2017) Dynamics and Control of Quadcopter Using Linear Model Predictive Control Approach. *IOP Conference Series*: *Materials Science and Engineering*, **270**, Article 012007. https://doi.org/10.1088/1757-899x/270/1/012007

[15] Suthanthira Vanitha, N., Manivannan, L., Meenakshi, T. and Radhika, K. (2020) Stability Analysis of Quadrotor Using State Space Mathematical Modeling. *Materials Today*: *Proceedings*, **33**, 4040-4043. https://doi.org/10.1016/j.matpr.2020.06.428

[16] Elharati, H.A., Alharati, S.A., Wareg, Z.O. and Waregh, M.A. (2023) Design Optimization for Generating a High Static Magnetic Field. *World Journal of Engineering and Technology*, **11**, 793-806. https://doi.org/10.4236/wjet.2023.114054